Korean Journal of Remote Sensing, Vol.21, No.1, 2005, pp.15~29

Efficiency of Superconducting Gravimeter Observations and Future Prospects

Juergen Neumeyer

GeoForschungsZentrum Potsdam, Dept. Geodesy and Remote Sensing, Telegrafenberg, 14473 Potsdam, Germany

Abstract : Superconducting Gravimeters (SG) are the most sensitive instruments for measuring temporal gravity variations. The gravimeter is an integrating sensor therefore the gravity variations caused by different sources must be separated for studying a special effect by applying different models and data analysis methods. The present reduction methods for gravity variations induced by atmosphere and hydrosphere including the ocean and the detection and determination of the most surface gravity effects are shown. Some examples demonstrate the combination of ground (SG) and space techniques especially the combination of SG with GRACE satellite derived temporal gravity variations. Resulting from the performance of the SG and the applied data analysis methods some proposals are made for future SG applications.

Key Words : Superconducting Gravimeter, Temporal Gravity Variation, Surface Gravity Effects, Space Techniques, GRACE, GPS.

1. Introduction

The Superconducting Gravimeter (SG) is an integrating sensor measuring gravity variations associated with mass redistributions in its near and far surroundings. Therefore, the recordings include temporal gravity variations of different sources.

Because matter has the properties of gravity and inertia, the sensor inside the gravimeter (a test mass) reacts to time variations of:

a) Gravitational forces (Newtonian attraction) caused by redistributions and density variations of all surrounding masses and

b) Inertial forces caused by accelerations, i.e., the second time derivative of the vertical position of the gravimeter site.

The gravimeter integrates gravity changes of different sources and cannot separate them. These separations can be done by applying different models and data analysis methods.

In most cases research is concentrated on global gravity effects such as Earth tides, seismic normal modes, core modes, Nearly Diurnal Free Wobble (NDFW), Chandler wobble etc. To investigate one special effect, all the other parts have to be removed from the gravity data. The other parts are disturbing signals in this case.

One disturbing part consists in accelerations (vibrations) usually considered as noise (seismic, industrial and ocean noise), which can be reduced by

Received 10 December 2004; Accepted 20 January 2005.

low- or band-pass filtering (if the particular frequencies are known). Supplementary instrumental effects (drift, offsets and instrumental noise) superimpose the gravimeter signal. Most of these effects can also be removed from data. Another part usually treated as disturbing signals are environmental influences. To remove them, they have to be modelled and hence the environmental parameters of the atmosphere and hydrosphere (e.g. atmospheric pressure, groundwater table, precipitation etc.) must be measured precisely. As better the different gravity effect can be modelled and reduced, as better one special effect can be investigated.

2. SG Performance Parameter

The Superconducting Gravimeter performance is shown in Table 1. The SG is characterized by a resolution better than 1ngal ($10^{-11}ms^{-2}$) a period range from seconds to years with a linear transfer function and a linear drift rate of about 3μgal/yr. The new instruments do not need liquid Helium refilling. In a closed circuit the He Gas is liquefied by a compressor. The dual sphere SG has the same parameters for each sensor as the single sphere SG. Additionally the dual sphere system measures the gravity gradient with a resolution of about 0.5μgal/m (5 Eötvös).

Fig. 1 shows the noise spectrum expressed as power spectral density (PSD) and noise magnitude $NM=10 \cdot \log(PSD)$ in dB for the Sutherland SG site in South Africa. A comparison between the Noise Magnitude and the New Low Noise Model shows that the Noise Magnitude characterizing the quality of the site is close and even smaller as the New Low Noise Model values at frequencies below 1mHz. This comparison emphasizes that the site offers excellent conditions for high precision gravity measurements and the detection of weak gravity signals. In this frequency range the free

Table 1. Superconducting Gravimeter Parameters.

Resolution ADC (24bit)	$10^{-12}ms^{-2}$
Resolution gravity	$>10^{-11}ms^{-2}$
Period range	10s - yrs
Measurement range	0.001ngal to 1.5mgal
Accuracy calibration factor	0.2% ~0.05μgal/Volt
Gravity phase shift (standard)	8.6s (0.035deg/cpd)
Gravity filter corner frequency (standard)	61.5mHz
Drift rate	~ 3μgal/yr

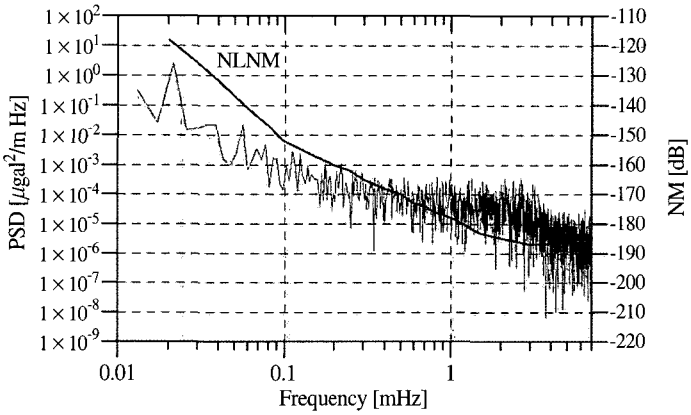

Fig. 1. Noise spectra at Sutherland SG site. Grey: Power Spectral Density (PSD) and Noise Magnitude (NM) of lower SG sensor. Black: New Low Noise Model (NLNM).

oscillations of the Earth have their modes too. Therefore they can be detected very well.

3. Global Surface Gravity Effects

Table 2 summarizes the main global surface gravity effects which the SG records. All these effects are included in the raw gravity data. Depending on the SG site, additional local effects can contribute to the gravity signal mainly caused by the hydrosphere and local secular gravity variations from postglacial rebounds, post seismic deformation, crustal deformation in tectonic active zones etc.

Measuring and analysing of these effects is now directly addressed to the "Global Geodynamic Project" (GGP) (Crossley, 2004). A network of 20 worldwide distributed stations equipped with Superconducting Gravimeters in operation since July 1997, using a similar hardware and the same procedures for data acquisition.

4. Data Processing and Reduction Methods

From the raw gravity data instrumental effects (spikes, steps, drift) must be removed. Data filtering is performed according to the period range of the gravity effect, which shall be investigated. The filters must be from type zero phase shift, to avoid a phase shift on the data. Only the instrumental gravity phase shift (0.036deg/cpd for the Sutherland SG station) must be applied on the data. The damping of the filter must be adapted to the resolution of the ADC. For a ADC resolution of 24 bit, the damping of the filter must be 140 dB. For preprocessing of the raw data the programs Tsoft (Tsoft, 2003) and PRETERNA (Wenzel, 1996) are capable tools for data repair and filtering. Before analysis of a special gravity effect (e.g. Earth tides), the gravity effects caused by the atmosphere, hydrosphere and the ocean are normally removed from the data.

1) Atmospheric Pressure Effect

The continual redistribution of air masses in the Earth's atmosphere causes temporal gravity variations. These variations highly correlate with the atmospheric pressure variations that can be measured and used for calculating the gravity effect. The frequency range of the ground atmospheric pressure changes varies from minutes to years and may reach up to 60hPa, which causes about 20μgal gravity variations. The redistribution of air masses affects the gravimeter sensor

Table 2. Global surface gravity effects.

Period range	Physical source	Gravity effect
0.1s - 10s	Micro seismic (natural or man made) Noise	up to ~10μgal
0.1s - 100s	Earthquakes	up to ~1mgal
1min - 1hr	Earth's free oscillation	< 1μgal
4hr - 8hr	Slichter modes	< 0.01ngal
6hr - 1yr	Body Tides	up to ~300μgal
6hr - 1yr	Tidal ocean loading	up to ~10μgal
hr - yr	Non-tidal ocean loading	up to ~1μgal
~430day(~15deg/h)	Earth's Nearly Diurnal Free Wobble (NDFW)	
min - yr	Atmospheric pressure variations	up to ~20μgal(~0.3μgal/hPa)
min - yr	Groundwater variations	~1-10μgal/m
~ 435day	Polar motion	up to ~10μgal

in two different ways:

1. Gravity changes due to the direct attraction of the air masses (attraction term, rough estimation - 0.43μgal/hPa (Torge, 1989).

2. Gravity changes due to vertical displacement of the gravimeter on the deformed Earth and the redistribution of masses caused by deformation (elastic deformation term, rough estimation 0.13μgal/hPa).

The deformation term acts in opposite direction to the dominant gravitational effect (attraction term). The accurate modelling of the attraction and deformation terms requires the knowledge of:

- Air density distribution in space and time.
- Atmospheric loading distribution in combination with a suitable regional Earth model.

In the past different methods for correcting atmospheric pressure effects were developed, which generally fall into two categories: empirical and physical approaches. The empirical approaches use the regression (single admittance) and the cross spectral density (frequency dependent admittance) analysis between local atmospheric pressure and gravity (Warburton and Goodkind, 1977; Crossley *et al.*, 1995; Neumeyer, 1995). The physical approaches (Merriam, 1992; Sun, 1995; Kroner, 1997; Neumeyer *et al.*, 1998) based on atmospheric models determine the attraction and deformation terms according to Green's function with 2D atmospheric pressure data and a standard height-dependent air density distribution. The empirical approaches yield good reduction results in a periodic range from minutes to days (for free oscillation up to the short-period tidal band). A small improvement of the reduction can be obtained with the 2D model in the long-periodic tidal band.

The 3D model considers the real height-dependent density distribution in the atmosphere for calculation of the attraction term. The deformation term can be calculated with 2D data according to the Greens loading function with adequate precision.

From European Centre for Medium-Range Weather Forecasts (ECMWF) global 3D atmospheric pressure data are available with a spacing of 0.5 degree up to 60 km height and an interval of 6 hours. These data can be applied for calculation of the atmospheric attraction term *gattr* due to formula (1) with γ = gravitational constant, ρ = density of the air segment, R_{GS} = Earth radius at the gravimeter station, $r = R_{GS}$ + height of the spherical air segment sV, θ_{RS} = co-latitude gravimeter site, λ_{RS} = longitude gravimeter site, θ and λ = coordinates sV.

$$gattr_{l,m,n} = -\gamma\left[\sum_{l,m,n} \rho_{l,m,n}\, sV_{l,m,n}\, A_{l,m,n}\right] \qquad (1)$$

$$A_{l,m,n} = \frac{R_{GS} - r_l[\sin \upsilon_{GS} \sin \upsilon_m (\cos \lambda_{GS} \cos \lambda_n + \sin \lambda_{GS} \sin \lambda_n) + \cos \upsilon_{GS} \cos \upsilon_m]}{\{R_{GS}^2 + r_l^2 - R_{GS} r_l[\sin \upsilon_{GS} \sin \upsilon_m (\cos \lambda_{GS} \cos \lambda_n + \sin \lambda_{GS} \sin \lambda_n) + \cos \upsilon_{GS} \cos \upsilon_m]\}^{3/2}}$$

By applying the 3D attraction model (Neumeyer *et al.*, 2004a) it could be shown that the gravity variations induced by mass redistribution in the atmosphere include a surface pressure-independent part (SPI) in the order of 1-2 μgal between summer and winter tine. This part can only be determined by using 3D atmospheric pressure data. From this results, the gravity reduction for analysing longperiodic gravity variations (long-periodic tidal waves, pole tide, hydrological effects) will be improved by applying the 3D attraction model. The same improvement can be expected for the reduction of absolute gravity measurements or the comparison of gravity measurements at different seasons.

For more precise calculations the 3D atmospheric pressure data should have a spacing of about 0.1 deg, an interval of 1hr and a better accuracy. This can be achieved with the satellite occultation technique in future. Fig. 2 shows an example of the SPI part at the same ground pressure of 905.25 +/- 0.25 hPa for the Matsushiro SG station in Japan.

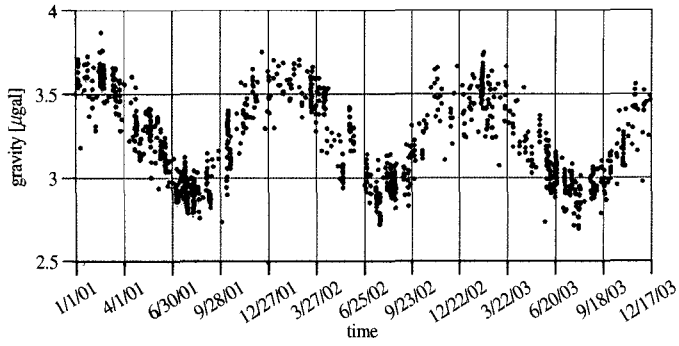

Fig. 2. Surface pressure independent gravity variations (SPI) at surface pressure 905 +/-0.25 hPa at SG station Matsushiro, Japan.

2) Ocean Loading

The ocean gives rise to noise at the site and causes the ocean loading effect. By low-pass filtering, the ocean noise can be drastically reduced. The ocean loading can be modelled and adjusted for the tidal parameters according to a suitable ocean model.

The researches show that the influence of the ocean tides on gravity measurements is one of the main perturbations, therefore it is necessary to remove them completely as possible before they are used to the study of other geophysical and geodynamical phenomena. Based on the most recent global ocean models like NAO99b (Matsumoto *et al.* 2000) and FES2002 (Le Provost *et al.* 2002), the gravity loading vectors for various tidal waves can be calculated with the program LOAD97 (Francis and Mazzega, 1990), After removing the oceanic load vector $\vec{L}(L, \lambda)$ from observed residuals $\vec{B}(B, \beta)$ the remaining final residual $\vec{X}(X, \xi)$ is still significant for different waves.

$$X_i = [B_i^2 + L_i^2 - 2B_iL_i(\beta_i - \lambda_i)]^{1/2}$$
$$\xi_i = \tan^{-1}[(B_i \sin \beta_i - L_i \sin \lambda_i)/(B_i \cos \beta_i - L_i \cos \lambda_i)] \quad (2)$$

The analysis demonstrates (Sun *et al.*, 1999) that the main reason for this are the load vectors $\vec{L}(L, \lambda)$ which are not well determined due to the inaccuracy of the global ocean models, the lack of the regional ones and the sometimes complicated bay coastal lines, which induce a kind of special shallow sea tidal phenomena. This means the global ocean models do not reflect well the real oceanic tidal phenomena. The remaining residual vector $\vec{X}(X, \xi)$ after ocean correction can be in the order of some μgal for the main tidal waves depending on the SG location (e.g 1.8μgal for M2 at SG station Sutherland). To improve the loading correction and reduce the discrepancy between observed and predicted ones, additional tide gauge measurements can increase the correction. In Neumeyer *et al.* (2005a) analysis results are shown with additional tide gauge measurements. Here the additional tide gauge corrected tidal parameters are much closer to the WD model tidal parameters to those compared with ocean model correction only. Through this the discrepancy between global oceanic loading corrected Earth tide parameters and theoretical predictions is reduced up to 4%. The improvement of the additional tide gauge correction can not only be seen in the semidiurnal and diurnal tidal band, but also in the observed tidal gravity residuals at higher frequencies. Fig. 3 shows the efficiency of the ocean loading correction with additional tide gauge measurements (TG) at gravimeter station Baconao near Santiago de Cuba.

3) Hydrology

The water circulation in the surroundings of the

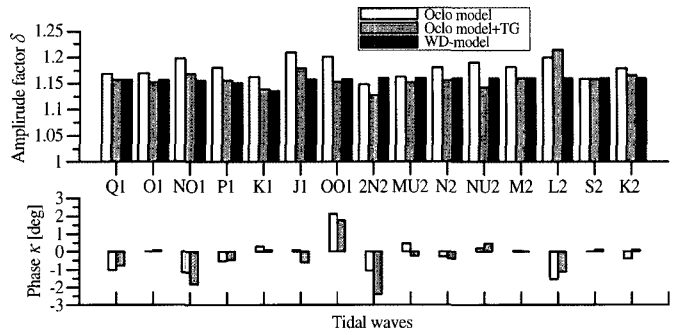

Fig. 3. Earth tide amplitude factors and phase analysed with different ocean loading corrections in comparison with the Wahr-Dehant model (from Neumeyer *et al.*, 2005a) (black = WD-model, white = NAO99b & FES2002 (Oclo model), grey = NAO99b & FES2002 and additional local ocean loading (Oclo model + TG)).

gravimeter causes variation by gravitational attraction and deformation at the surface similar to that due to the atmosphere. Precipitation (rain and snow) at the surface causes changes in soil moisture and groundwater level. One part of this precipitation evaporates at the surface and in the ground. Another part increases the groundwater level or drains off.

Presently most of the SG stations are equipped with a borehole for measuring groundwater level variations. In many cases a good correlation between gravity and groundwater level variations could be shown (Kroner, 2001). The gravity effect of these variations is determined in most cases with the regression analysis. The regression coefficient is varying between about 1 - 10 μgal/m depending on the hydrological conditions. This is a simple model, which reflects the real hydrological gravity signal not very accurately. For better modelling a local hydrology model is necessary around the SG site, which considers the local hydrological cycle. Input data for this model should be precipitation, soil moisture and groundwater level variations measured at representative locations for this model. With such a model the local gravity variations induced by the hydrosphere can be evaluated satisfactory.

For modelling of gravity variations derived from global hydrology models the following are available: WGHM: University of Kassel, (Doll *et al.*, 2003); H96: Climate Prediction Center (NOAA), (Huang *et al.*, 1996); LaD: U.S. Geological Survey (USGS), (Milly and Shmakin, 2002). These models have a spatial resolution of 0.5 degree and a temporal resolution of 1month. The data represent changes in terrestrial water storage expressed in equivalent water thickness. This term can be expanded into spherical harmonics, transformed into potential coefficients (e.g. up to degree l_{max}=10) and then used for calculating of the gravity changes at the SG location (Neumeyer *et al.* 2005b). Fig. 4 shows the gravity variations derived from different hydrology models for SG station Moxa, Germany, which are used for comparison with SG measured and GRACE derived gravity variations.

5. Analysis of Global Surface Gravity Effects

The Earth tides are the largest signal in the gravity recordings. For analysing three programs ETERNA (Wenzel, 1996) VAV2002 (Venedikov *et al.*, 2001) and

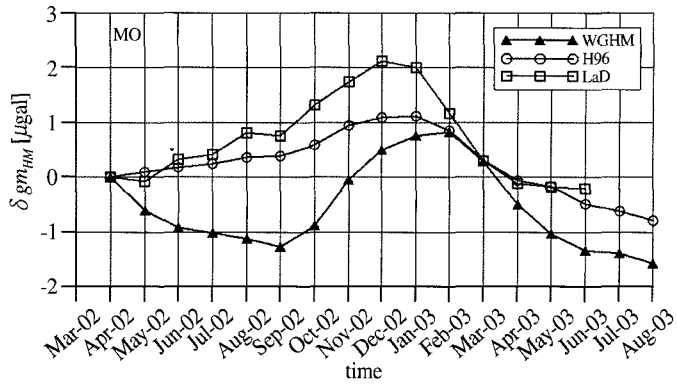

Fig. 4. Gravity variations derived from hydrology models WGHM, H96 and LaD (l_{max} = l0 at the SG-site Moxa, Germany (from Neumeyer *et al.* 2005b).

BAYTAB-G (Tamura, 1990) are in use. All three programs deliver results within the same error bars (Dierks and Neumeyer, 2002). The ETERNA program is based on the least square method using the Wahr-Dehant tidal model and different tidal potential catalogues. The most accurate catalogue is the HW95 with a resolution of 1ngal (Hartmann and Wenzel, 1995).

The high precision estimation of the gravitational amplitude factor δ and phase κ for the different partial tidal waves, which represent the response of the Earth body to tidal forces are mainly used for:

- Earth tide reduction for relative and absolute gravity and other precise measurements like satellite positioning, GPS-, Laser-, radio-interferometric methods
- Investigation of global Earth and Earth tide models
- Investigation of changes of the tidal parameters
- Determination of the resonance effect of the liquid core (Nearly Diurnal Free Wobble)
- Verification of the Love numbers h and k by gravity (SG) and GPS measurements
- Verification of global and regional oceanic tide models (Baker and Bos, 2003).

The accuracy of the tidal parameters depends on the SG calibration accuracy and the reduction of the other gravity effects in this period range (atmosphere, hydrology and ocean). With an calibration accuracy of 0.2% the tidal factors can be determined to $\Delta\delta$ = +/- 0.002. The phase shift of the SG can be determined with an accuracy better than 1s. From this follows the phase lead can be determined better than 0.01 deg for the diurnal tidal waves.

Fig. 5 shows the determined tidal parameters based on Sutherland SG recordings. For comparison the Wahr-Dehant model (white columns) and the observed amplitude factors (gray columns) are pictured. The deviations from the model can be seen clear. One reason for the deviations is the influence of the ocean loading. Therefore the ocean loading correction has been calculated for the diurnal partial tides Q1, O1, P1 and K1 and the semidiurnal partial tides N2, M2, S2 and K2. The black columns show the ocean loading corrected amplitude factors. One can see that the ocean loading corrected amplitude factors come closer to the model values for the semidiurnal waves N2, M2, S2, K2 and the diurnal waves P1 and K1. For the diurnal waves Q1 and O1 the ocean loading corrected amplitude factors depart form the model values. The reason for this behavior is the ocean loading model also shown in

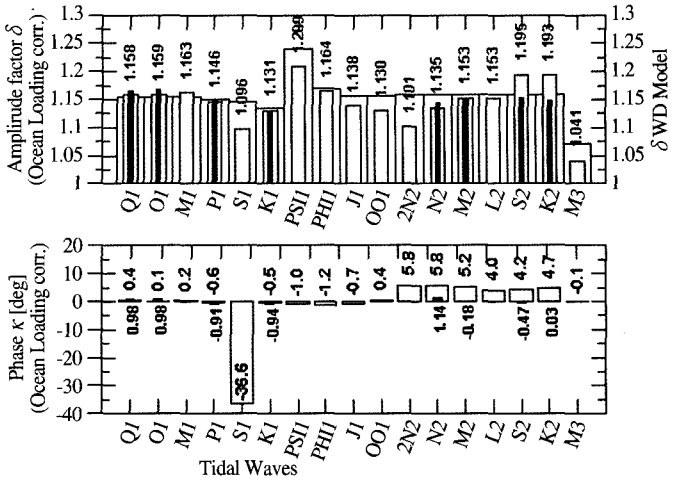

Fig. 5. Earth tide parameters δ and κ for SG station Sutherland, South Africa. White columns: Wahr-Dehant model parameter δ; Gray columns: calculated parameters δ and κ; Black columns: Ocean loading corrected parameters δ and κ.

Ducarme *et al.* (2002).

The model phase is zero. Larger deviations from the model phase show the semidiurnal waves 2N2, N2, M2, L2, S2, K2 and the diurnal wave S1. The ocean corrected phase leads for the diurnal waves N2, M2, S2 and K2 give a good improvement close to zero (observed values near 5 deg phase lead). The ocean corrected phase lead for the diurnal waves Q1, O1, P1 and K1 become larger than the uncorrected value. The strong deviation (δ and κ) of the S1 wave to the model may be caused by the influence of the daily variations of the atmospheric pressure, which are not corrected completely.

The Nearly Diurnal Free Wobble (NDFW) is a small retrograde motion of the Earth instantaneous rotation axis about the figure axis, connected with the Free Core Nutation (FCN) a retrograde motion of the rotation axis in space. The figure axis of the mantle and the rotation axis of the elliptical fluid core are mis-aligned mostly due to an interaction with the core mantle boundary. The reaction of the rotating core and mantle results in a nutation in space and a wobble with respect to the Earth fixed axis.

The NDFW resonantly amplifies nearly diurnal tides and annual and semi-annual nutation. The tides which are mostly affected are P1, S1, K1, Psi1 and Phi1. Their amplitudes are influenced, because they are close to the eigenfrequency of the NDFW. With the GGP network the eigenfrequency of the NDFW has been determined between 429.1 and 429.9 days (Ducarme *et al.*, 2002). It is close to the Methew model (Methews *et al.*, 2002) of 430.04 days

The main components of the polar motion are a free oscillation (Chandler Wobble) with a period at 435 days and an annual oscillation, which is mainly forced by the seasonal mass redistribution in the atmosphere an the oceans. The recording of the polar motion is curried out with VLBI, LLR, SLR and GPS measurements. The International Earth Rotation Service IERS provides a smoothing of these measurements with a resolution of 1day. The polar motion causes changes in centrifugal acceleration, which can be measured by the SG. From the IERS polar motion data X(t) and Y(t) the gravity effect of the polar motion can be calculated for the SG

station with colatitude θ and longitude λ according to formula (3) (Torge, 1989)

$$\Delta g_{pol}(\theta,\lambda,t) = R\Omega^2\delta_{pol}\sin(2\theta)\cdot(X(t)\cos(\lambda) - Y(t)\sin(\lambda)) \quad (3)$$

with R = Earth radius, Ω = angular velocity of the Earth and $\delta_{pol} = 1.16$.

For mid latitudes $\theta = 45°$ Δg_{Pol} has a maximum. The polar motion derived from the IERS data can be used for comparing with SG measurements. Some of the SG stations deliver very similar results like the IERS observations. The determined δ_{Pol} factor ranges from 1.1 to 1.18. For some stations it is close to the Wahr-Dehant model value of 1.16 (Hinderer and Crossley, 2000; Harnisch and Harnisch, 2004). Fig. 6 shows the polar motion measured with the SG at Sutherland site in comparison with the calculation from IERS data.

By a large Earthquake the Earth is set into its natural oscillations (Earth's free oscillation). This oscillation is free and there are two independent types:

- Toroidal oscillations (T): The displacement for toroidal oscillations is always perpendicular to the radius vector. These oscillations involve only the crust and mantle. They are equivalent to all the Love waves.
- Spheroidal oscillations (S): The displacement for spheroidal oscillations has both radial and tangential components. They are equivalent to all the Rayleigh waves.

Both types of oscillations have an infinite number of modes. The SG can clearly detect the S modes. Below 0.6 mHz the SG has the highest signal to noise ratio and it produces the best spectra and splitting of these modes (especially 0S2, 2S1 and 0S3). Based on this splitting the 3-D density structure in the Earth's mantle and core can be investigated (Widmer-Schidrig, 2003). Fig. 7 shows an example of the free oscillation after the Peru earthquake (latitude 16.14S, longitude 73.312 W, depth 33 m,) on June 23rd 2001 at 20:33:14.14 with a magnitude of 8.4.

Slichter (1961) first pointed out that some of the Earth's free oscillations might consist principally of translational oscillations of the inner core about its equilibrium position at the centre of the Earth. Unlike Earth's other free oscillations, the restoring force on the inner core is primarily gravitational than elastic. Due to the Earth's rotation, a single mode is split into three different polarisations (the Slichter triplet): one along the axis of rotation and two in the equatorial plane (one prograde and one retrograde with respect to the sense of the Earth's rotation). Of all Earth's free oscillations, perhaps the translational motions of the solid inner core are the most exclusive. The signal of these oscillations at

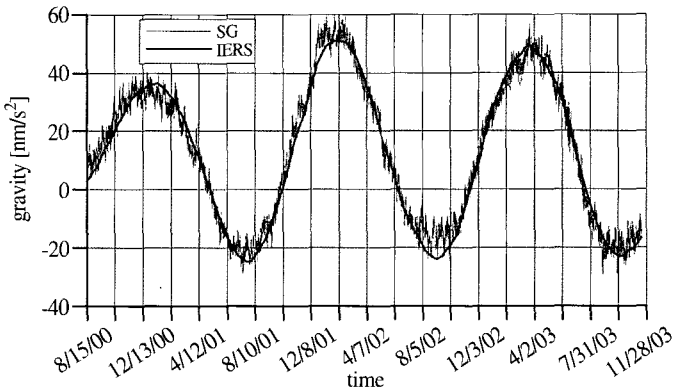

Fig. 6. Polar motion measured with the SG at Sutherland site and calculated from IERS data.

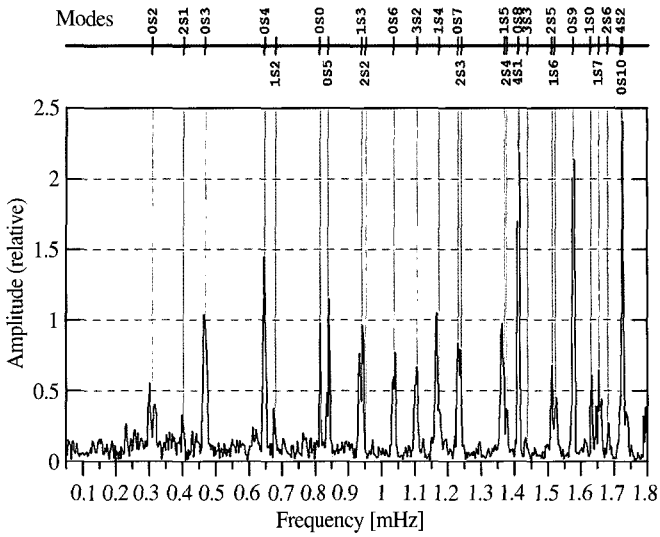

Fig. 7. Spheroidal free oscillation modes after the Peru earthquake on June 23rd 2001.

the Earth's surface will be a small periodic change in gravity below the ngal level. Observational identification depends on the detection of all three distinct periods in time series from different sites.

The periods of the Slichter triplet are very sensitive to deep interior properties (e.g. the density jump at ICB, viscosity of outer fluid core) hence credible observational identification provides valuable information about the Earth's inner structure. Up to now the Slichter triplet is not yet detected with high significance. Different figures have been published (Rosat *et al.*, 2004). The SG network is the only configuration for detecting the Slichter triplet.

6. Combination of Ground (SG) and Space Techniques

1) Combination of SG and GPS Measurements

The GPS technique can achieve a positioning precision in mm range for displacement variation (height variation) of a point on the Earth's surface e.g. for the SG site. To get this precision, one needs a GPS network in minimum of two stations. One station is the reference station, which is considered as fixed and error free and the coordinate variations of the other station, which is located at the SG site can be determined. Adding more reference stations can improve the precision of the result. The coordinates of the reference station must be known before processing better than 1cm. This can be achieved by using data of the IGS (International GPS Service) GPS network or using of IGS stations as reference stations. The distance between the GPS stations should be between 100km and 800km approximately. The minimal observation time should be a few days. This is a short time compared to the much larger time span needed for comparing with SG measurements. The precision in mm range you will get with a static GPS solution only. If you select a dynamic solution the precision only will be in cm range (Xu, 2003). The comparison between SG and GPS measurements offers the separation of gravity variations caused by vertical displacements and the associated

mass redistributions. In Zerbini *et al.* (2001) you find good correlations between gravity and GPS measured height variations.

2) Combination of Satellite Derived Gravity Variations with SG Measurements

One objective of the new-generation satellite gravity missions CHAMP and GRACE is the recovery of temporal Earth gravity field variations. Of fundamental interest is the combination of satellite-based and ground gravity measurements. Because GRACE's temporal resolution ranges from 1month to years, ground gravity measurements must have a long-term stability, which only Superconducting Gravimeters fulfil. In Neumeyer *et al.* (2004b) could be proven that SG (point) measurements are representative for a large area, if the local gravity effects are removed.

For the GRACE mission the gravity resolution Δgres is about 0.5 μgal at a half wavelength spatial resolution of $\lambda/2$ = 2000 km which corresponds to the spherical harmonic coefficients up to degree l_{max} = 10. The temporal resolution is 1month. For a satellite the gravity resolution is connected with the spatial resolution. With higher degree l the gravity resolution decreases and the spatial resolution becomes finer. For comparison with SG measurements monthly solutions up to l_{max} = 20 (Δgres ~ 2.5 μgal and $\lambda/2$ ~ 1000 km) can be applied.

Preconditions for the combination of satellite derived and ground measured gravity variations are:

- Reduction oft the same gravity effects in both data sets (SG and GRACE) under use of the same models. Both data sets must represent the same sources of gravitation and the same spatial resolution. Therefore all local gravity effects must be removed from the ground measurements.
- In contrast to the SG the satellite is not coupled to the Earth surface and therefore not sensitive to a vertical surface shift (height variation). It is described by the body Love numbers h_l and the loading Love numbers h'_l. This fact must be considered for reducing of the different gravity effects.

In Fig. 8 (Neumeyer *et al.*, 2005b) are shown comparison results between GRACE, selected SG stations and hydrology models. The GRACE recovery of temporal gravity field variations is performed by monthly solutions for the SG locations from sets of spherical harmonic coefficients up to l_{max} = 20. The following reductions are applied:

- Earth tides: based on IERS Earth tide model applied from semidiurnal to long period constituents.
- Ocean tides and ocean loading: based on FES2002 ocean tide model from semidiurnal to long period constituents.
- Pole tide: based on IERS polar motion data.
- Air pressure effect (attraction and loading term): based on 3D air pressure model with 6 hourly ECMWF data.

In comparison with the SG the satellite is not sensitive for a height variation caused by a loading. To compare both measurements the gravity variations caused by this effect and described through the load Love number h'_l are added to the monthly GRACE solutions. The Love numbers h'_l are considered in the gravity calculation from the spherical harmonic coefficients.

From the raw SG gravity data spikes, offsets and drift are removed. At this continuous time series of hourly gravity variations the same gravity reductions are applied as for the GRACE processing. Additional the local groundwater level effect is removed.

The reduction of the gravity effect caused by the local hydrology possibly raises some problems. If the hydrology signal is a very local one, we must correct the effect. If the local hydrology effect contains components of the global hydrology, we would reduce the signal we want to compare. It is difficult to distinguish between local and global hydrological signals.

After the applied gravity reduction all gravity effects are reduced with the exception of that one of the hydrology. Therefore gravity variations derived from global hydrology model WGHM (Döll *et al.*, 2003) were used for comparing with resulting hydrological effects of GRACE and SG observations.

The comparison between GRACE, SG and global hydrology model derived gravity variations show a noticeable agreement, excepted for SG underground stations. For these stations the modelling of the hydrological effect above the station is difficult and not very accurate.

The comparison results give suggestions for further investigations of each data series. For better modelling of the local gravity effect, induced by the hydrosphere, all SG sites should be equipped with ground water table, soil moisture and rain gauges which are inputs for a local hydrological model around the SG station. The comparison result shows furthermore SG measurements of the GGP SG network can contribute to validate GRACE and further gravity satellite missions. In addition field SG measurements should be carried out for further validation in areas with large or very small gravity variations e.g. the Amazon area, where seasonal gravity changes can be observed in the order of some 10 μgal or in the Atacama desert with a very small hydrological signal.

One example of comparison is displayed in figure 8. It shows the gravity variations δgm_{SG} derived from SG, GRACE (solutions from GFZ Potsdam and Centre Space Research University of Texas at Austin (CSR)) and hydrology model WGHM. The error bars at the SG graph do not represent measurement errors they show the variations of gravity within this month. All curves show a good agreement within their estimated error bars.

7. Future Applications

Besides measuring of the global gravity effects the SG also can be used for measuring special regional and local gravity effects, because it is possible to remove all the other effects from the data, which can be well separated by special analysis and modelling methods. Some examples and proposals are:

- Measuring of local hydrology signals for solving interesting hydrologic questions like area-averaged water storage, storage change, infiltration time, aquifer heterogeneity etc. The project of the University of Austin will measure the hydrological signal with a transportable SG at different places at the Edwards Aquifer of Central Texas (Wilson *et al.*, 2004).

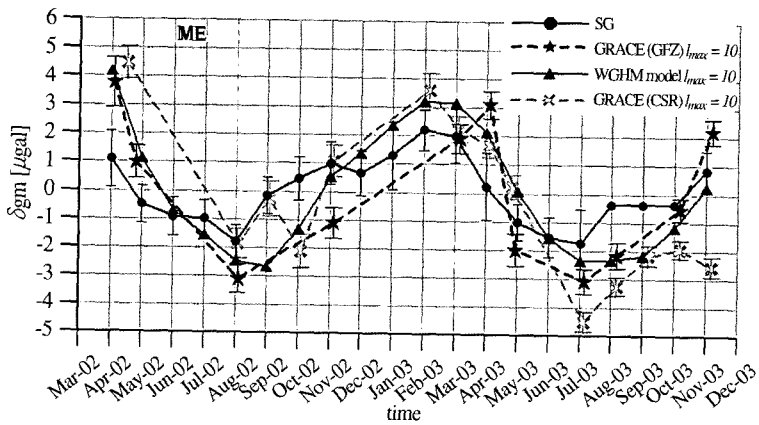

Fig. 8. Gravity variations δgm for SG site Metsahovi, Finland (from Neumeyer *et al.*, 2005b).

- Volcano observations a combination of SG and GPS measurements for detecting mass transport (mass redistribution) and through this caused ground deformation. By combination of both measurements a separation of mass transport (SG) and deformation (SG and GPS) is possible. The deformation can be determined with GPS stations in mm range. A correlation of the combined signal (SG and GPS) with seismic, electromagnetic, chemical measurements etc. can yield new information.
- Mass transport and crustal deformation in tectonic active zones
- Detection of silent earthquakes by a combination of SG, GPS and seismic measurements. For instance in the Cascadian subduction zone, where displacements in cm range have been observed (Rogers and Dragert, 2003).

8. Conclusions

The present measuring and modelling precision including the separation of the different global and local gravity effects is sufficient for SG based investigation of regional gravity effects such as secular gravity variations from postglacial rebounds, post seismic deformations, mass transport in tectonic active areas, hydrology signals, volcano activities, silent earthquakes etc.

References

Baker, T. F. and M. S. Bos, 2003. Validating Earth and ocean tide models using tidal gravity measurements, *Geophys. J. Int,*. 152: 468-485.

Crossley, D., O. G. Jensenand, and J. Hinderer, 1995. Effective barometric admittance and gravity residuals, *Phys. Earth Planet Int.*, 90: 221-241.

Crossley, D., 2004. Preface of the Global Geodynamic Project, *Journal of Geodynamics*, 38(3-5): 225-236.

Dierks, O. and J. Neumeyer, 2002. Comparison of Earth Tides Analysis Programs, *Bull. Inf.*, Marees Terrestres, 135: 10669-10688.

Doll, P., F. Kaspar, and B. Lehner, 2003. A global hydrological model for deriving water availability indicators: model tuning and validation, *J. Hydrol.*, 270: 105-134.

Ducarme, B., H., P. Sun, and Q. Xu, 2002. New Investigations of tidal gravity results from the GGP network, *Bull. Inf.*, Marees Terrestres, 136: 10761-10776.

Francis, O. and P. Mazzega, 1990. Global charts of ocean tide loading effects, *J. Geophys. Res.*, 95: 11411-11424.

Harnisch, M. and G. Harnisch, 2004. Study of long term variations based on data of the GGP co-operation, Present. at 15th Symp. On Earth Tides, Ottawa.

Hartmann, T. and H. G. Wenzel, 1995. The HW95 tidal potential catalogue, *Geophys. Res. Lett.*, 22(24): 3553-3556.

Hinderer, J. and D. Crossley, 2000. Time variations and interferences on the Earth's structure and dynamics Surveys, *Geophysics*, 21: 1-45.

Huang, J., H. M. Van den Dool, and K. P. Georgakakos, 1996. Analysis of model-calculated soil moisture over the United States (1931-1993) and applications to long-range temperature forecasts, *J. of Climate*, 9: 1350-1362.

Kroner, C., 1997. *Reduktion von Luftdruckeffekten in zeitabhängigen Schwerebeobachtungen*, Dissertation, Technische Universität Clausthal.

Kroner, C., 2001. Hydrological effects on gravity data of the Geodynamic Observatory Moxa, *J. Geodyn. Soc. Jpn.*, 47(1): 353-358.

Le Provost, C., F. Lyard, F. Lefevre, and L. Roblou,

2002. FES 2002 -A new version of the FES tidal solution series, *Abstract Volume Jason-1 Science Working Team Meeting*, Biarritz, France.

Merriam, J. B., 1992. Atmospheric pressure and gravity, *Geophys. J. Int.*, 109: 488-500.

Methews, P. M., T. A. Herring, and B. A. Buffett, 2002. Modelling of nutation precision: New nutation series for nonrigid Earth and inside into the Earth's interior, *J. Geophs. Res.*, 107(B4); ETG3-1: 3-30.

Milly, P. C. D. and A. B. Shmakin, 2002. Global modeling of land water and energy balances. Part I: The Land Dynamics (LaD) Model, *J. Hydrometeorology*, 3(3): 283-299.

Neumeyer, J., 1995. Frequency dependent atmospheric pressure correction on gravity variations by means of cross spectral analysis, *Bull. Inf.*, Marees Terrestres, 122: 9212-9220.

Neumeyer, J., F. Barthelmes, and D. Wolf, 1998. Atmospheric Pressure Correction for Gravity Data Using Different Methods, *Proc. 13th Int. Symp. on Earth Tides*, Brussels, 1997, Eds.: B. Ducarme and P. Paquet, pp.431-438.

Neumeyer, J., F. Barthelmes, L. Combrinck, O. Dierks, and P. Fourie, 2002. Analysis Results from the SG registration with the Dual Sphere Superconducting Gravimeter at SAGOS (South Africa), *Bull. Inf.*, Marees Terrestres, 135: 10607-10616.

Neumeyer, J., J. Hagedoorn, J. Leitloff, and T. Schmidt, 2004a. Gravity reduction with three-dimensional atmospheric pressure data for precise ground gravity measurements, *J. Geodyn.*, 38(3-5): 437-450.

Neumeyer, J., P. Schwintzer, F. Barthelmes, O. Dierks, Y. Imanishi, C. Kroner, B. Meurers, H. P. Sun, and H. Virtanen, 2004b. Comparison of Superconducting Gravimeter and CHAMP satellite derived temporal gravity variations, in *Earth observations with CHAMP* Eds.: C. Reigber , H. Lühr , P. Schwintzer, J. Wickert, Springer-Verlag, pp.31-36.

Neumeyer, J., J. del Pino O. Dierk, H. P. Sun, and H. Pflug, 2005a. Improvement of Ocean Loading Correction on Gravity Data with Additional Tide Gauge Measurements, Submitted to *J. Geodyn.*

Neumeyer, J., F. Barthelmes, O. Dierks, F. Flechtner, M.H. Harnisch, J. Hinderer, Y. Imanishi, C. Kroner, B. Meurers, S. Petrovic, C. Reigber, R. Schmidt, P. Schwintzer, H.-P. Sun, and H. Virtanen, 2005b. Combination of temporal gravity variations resulting from Superconducting Gravimeter recordings, GRACE satellite observations and global hydrology models, Submitted to *J. Geodesy.*

Rosat, S, J. Hinderer, D. Crossley, and J.P. Boy, 2004. Performance of Superconducting gravimeters from long-period seismology to tides, *J. Geodyn.*, 38(3-5): 461-476.

Rogers, G. and H. Dragert, 2003. Episodic tremor and slip on the Cascadia subduction zone: The chatter of silent slip, *Science*, 300: 1942-1943.

Slichter, L. B., 1961. The fundamental free mode of the Earth's inner core, *Proc. Nat. Acad. Sci.*, 47(2): 186-190.

Sun, H. P., 1995. *Static deformation and gravity changes at the Earth's surface due to the atmospheric pressure*, Observatoire Royal des Belgique, Serie Geophysique Hors-Serie, Bruxelles.

Sun, H. P., H. Hsu, S. Luo, and J. Xu, 1999. Study of the ocean models using tidal gravity observations obtained with Superconducting Gravimeter, *Acta Geodetica et Cartograophy Sinica*, pp.64-71.

Tamura, Y., 1990. *BAYTAP-G Users Manual*, Mizusawa National Astronomical Observatory.

Torge, W., 1989. *Gravimetry; de Gruyter*, Berlin, New York.

Tsoft, http://www.astro.oma.be/SEISMO/TSOFT/tsoft.html.

Venedikov, A. P., J. Arnoso, and R. Vieira, 2001. Program VAV/2000 for tidal analysis of unevenly spaced data with irregular drift and coloured noise, *J. Geodetic Society of Japan*, 47(1): 281-286.

Warburton, R. J. and J. M. Goodkind, 1977. The influence of barometric-pressure variations on gravity, *Geophys. J. R. Astr. Soc.*, 48: 281-292.

Wenzel, H. G., 1996. The nanogal software: data processing package Eterna 3.3, *Bull. Inf.*, Marees Terrestres, 124: 9425-9439.

Widmer-Schmidrig, R., 2003. What can superconducting gravimeters contribute to normal mode seismology?, *Bull. Seism. Soc. Am.*, 93(3): 1370-1380.

Wilson, C. R., J. Sharp, B. Scanlon, D. Pool, and T. Ferre, 2004. The Field Superconducting Gravimeter - A Hydro-geologic Sensor, Presentation at Int. Symp. on Gravity, Geoid, and Space Missions (GGSM2004), Porto, Portugal.

Xu, G., 2003. *GPS Theory Algorithms and Applications*, Springer-Verlag.

Zerbini, S., B. Richter, M. Negusini, M. Romagnoli, D. Simon, F. Domenichini, and W. Schwahn, 2001. Height and gravity variations by continuous GPS, gravity and environmental parameter observations in the southern Po Plain, near Bologna, Italy. *Earth and Planetary Science Letters*, 192: 267-279.